

## InGaP Visible Light Emitting Diodes on Si Substrates

Susumu Kondo, Shin-ichi Matsumoto and Haruo Nagai

NTT Opto-electronics Laboratories  
3-1, Wakamiya, Morinosato,  
Atsugi-shi, Kanagawa, 243-01, JAPAN

InGaP LEDs are successfully fabricated on Si substrates. InGaP p-n junctions are formed by MO-chloride VPE on GaAs and GaAsP buffer layers grown by a two step growth process involving atmospheric pressure MOVPE. 660 and 580nm light emissions occur by DC injection at room temperature. Optical and electrical characteristics of these LEDs show the feasibility of InGaP optical devices on Si substrates.

### 1. Introduction

Remarkable progress has been made in the fabrication of AlGaAs/GaAs devices on Si substrates, such as FETs,<sup>1)</sup> solar cells,<sup>2)</sup> LEDs and LDs.<sup>3)4)</sup> However, few attempts have been made with other III-V compound systems. This report describes the first successful fabrication of InGaP LEDs on Si substrates which emit at 660<sup>5)</sup> and 580 nm wavelength.

Visible LEDs on Si substrates<sup>6)7)</sup> are expected to have many applications, such as in LED arrays for printer heads, high contrast displays, and audio/video disk equipment. The direct band gap of ternary mixed crystal  $\text{In}_{1-x}\text{Ga}_x\text{P}$  ranges from 1.3 to 2.25 eV, and is about 1.9 eV at the composition lattice matched to GaAs ( $x \sim 0.5$ ). Recent developments in InGaAlP/InGaP visible region LDs have verified the usefulness of this material.<sup>8)</sup>

### 2. Crystal growth and characterization

MO-chloride VPE<sup>9)10)</sup> was used for InGaP layer growth. This technique has the same growth mechanism as that of conventional chloride VPE. However, III group metalorganic compounds are used instead of III group metals, and all sources are supplied in the

gas phase. This growth method does not include reactions between gases and molten metal sources, and reaction ambience can be changed rapidly. Therefore, this technique is suitable for growing mixed crystals with high composition control. The use of MO compounds leads to the possibility of carbon contamination of the grown crystals. The background impurity concentration of the undoped layer is on the order of  $10^{16} \text{ cm}^{-3}$ . With the MO chloride VPE, crystal quality is not as sensitive to growth conditions as with MOVPE, and InGaP of high optical quality and highly controlled composition can easily be grown.

Trimethylindium (TMI), Triethylgallium (TEG) and Phosphoric trichloride ( $\text{PCl}_3$ ) were used as sources of In, Ga and P, respectively. Diethylzinc was used as a p-type dopant.

Flat interfaces are necessary for fabrication of high quality p-n junctions. However, the surface morphology of VPE grown InGaP layers rapidly deteriorates with increasing lattice mismatch with the substrate. Thus, use of a buffer layer lattice matched to InGaP is necessary. In this study, GaAs and GaAsP layers were used

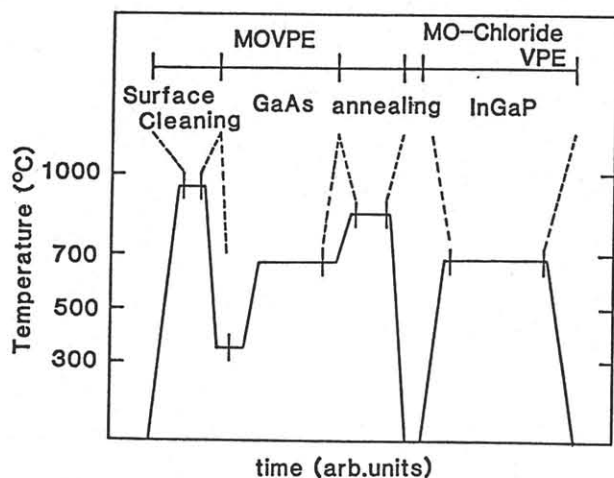


Fig.1 Schematic diagram of temperature schedule for InGaP LED wafer growth.

as the buffer layers for InGaP growth.

The temperature schedule for the growth of an InGaP LED wafer is shown in Fig.1. The n-type 2°off (100) Si substrate was heated to 1000°C for surface cleaning. GaAs or GaAsP layers were grown by a two step growth process involving atmospheric pressure MOVPE and were annealed at 850°C for 15 min. Then, n and p-type InGaP layers were grown by MO-chloride VPE.

The surface morphologies of InGaP layers grown simultaneously on GaAs and GaAs/Si substrates are shown in Fig.2. The as grown surfaces were macroscopically mirror like. However, fine structure was observed in the GaAs/Si with a Nomarski interference microscope.

The double crystal X-ray rocking curve for an InGaP/GaAs/Si wafer is shown in Fig.3. The full width of the half maximum from the InGaP layer ranges from 300 to 350 arcsec, and those from the GaAs layers from 200 to 270 arcsec. The molten KOH etching technique revealed a dislocation density of  $10^7 \text{ cm}^{-2}$  for the GaAs layer on the Si substrate. That of the InGaP layers is estimated to be of the same order.

### 3. InGaP LED

The structure of an InGaP LED on an Si substrate is shown in Fig.4. Circular and square mesa structures were formed by selective etching of InGaP layers by

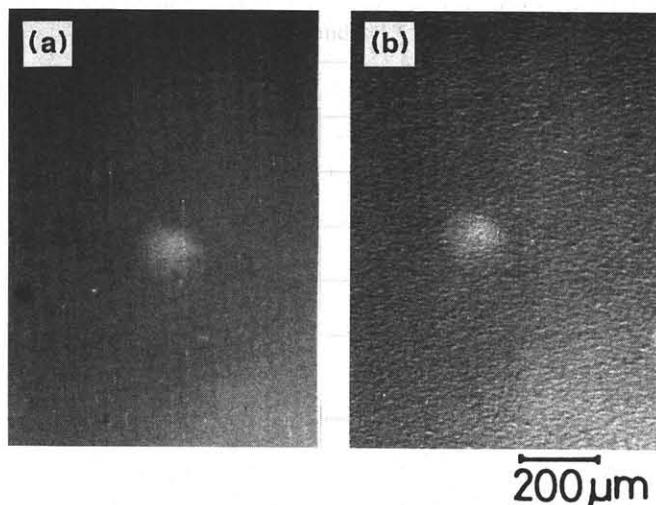


Fig.2 Surface morphology of InGaP layer. (a) on GaAs (b) on GaAs/Si

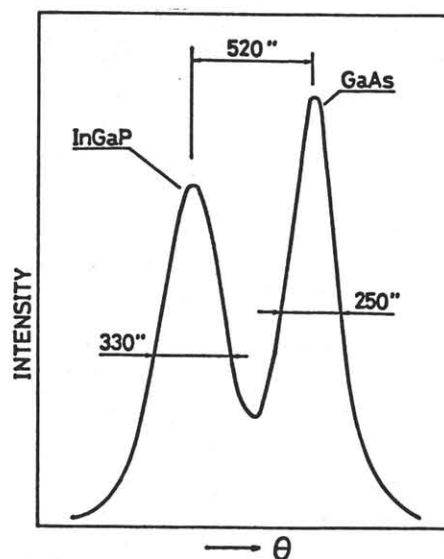


Fig.3 Double crystal X-ray rocking curves from InGaP and GaAs layers.

hydrochloric acid. Alloyed ohmic contacts to the p-InGaP layer and the n-Si substrate consisted of AuZn and AuGeNi. The carrier concentration of the n-InGaP layer was in the  $0.3-0.8 \times 10^{16} \text{ cm}^{-3}$  range, and that of the p-InGaP layer was about  $1 \times 10^{18} \text{ cm}^{-3}$ . The total thickness of the InGaP layers was about 2 μm.

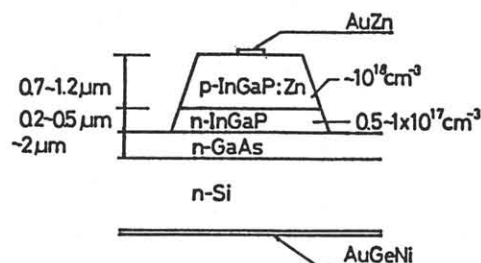


Fig.4 Cross-sectional view of an InGaP LED on a Si substrate.

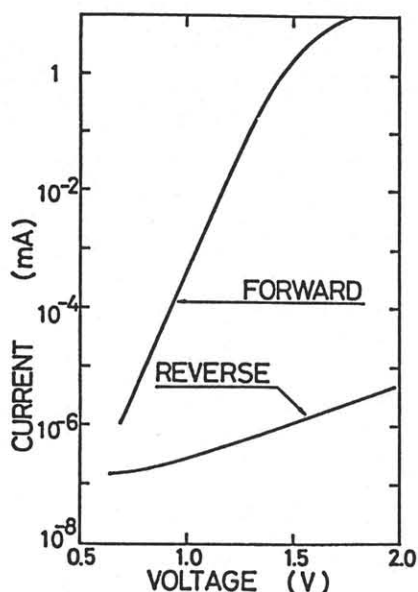


Fig.5 Voltage-current characteristics of InGaP LED on Si substrate.

The voltage-current (V-I) characteristics are shown in Fig. 5. The  $n$  value estimated from the small current region was 2. The capacitance-voltage measurements show that an abrupt p-n junction existed in the InGaP layer and that the built in voltage was 1.6 V.

The light emitting pattern from the array consists of 6 InGaP LED's is shown in Fig.6. Red light emission can be seen under room light with only 10 mA of injection current. The spectra under DC injection are shown in Fig. 7. The peak occurs at 660 nm with a half width of 25 nm.

Light output power was measured for LEDs with an epoxy lens, as shown in Fig. 8. The high density dislocations in the InGaP layers are thought to have a serious effect on quantum efficiency and reliability. Actually, dark spots are seen in electroluminescence patterns and EBIC images. On the other hand,

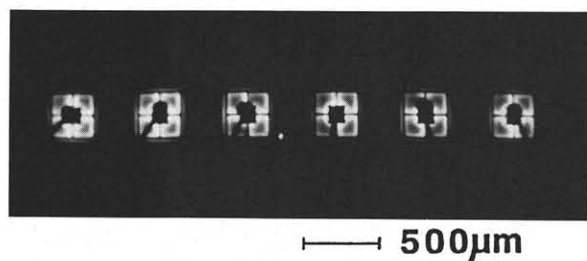


Fig.6 Light emitting pattern from LED array.

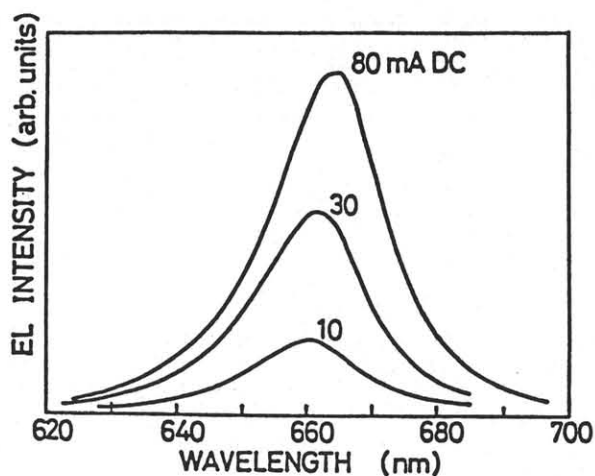


Fig.7 Emitting spectra of an InGaP LED on a Si substrate at room temperature.

for InGaP LEDs fabricated on the GaAs substrate, EL patterns and EBIC images are homogeneous without dark spots, and the output power level is about 1.5 ~ 2 times higher than those on Si substrates. Because the LEDs are still in the primitive stage, the device performance is considerably low even in the case of the LEDs on GaAs substrates. Improvement in these characteristics can be expected because LED output power is sensitive to device structure and crystal quality.

In spite of the existence of high density crystal defects, the LED operation was stable, and no rapid degradation was observed. The output power level and EL pattern did not change after 600 hours running under a DC injection current density of 500 A/cm<sup>2</sup>. No degradation was observed at

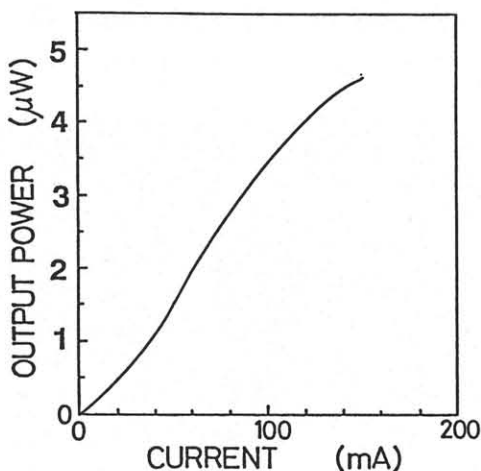


Fig.8 Current-output power characteristics

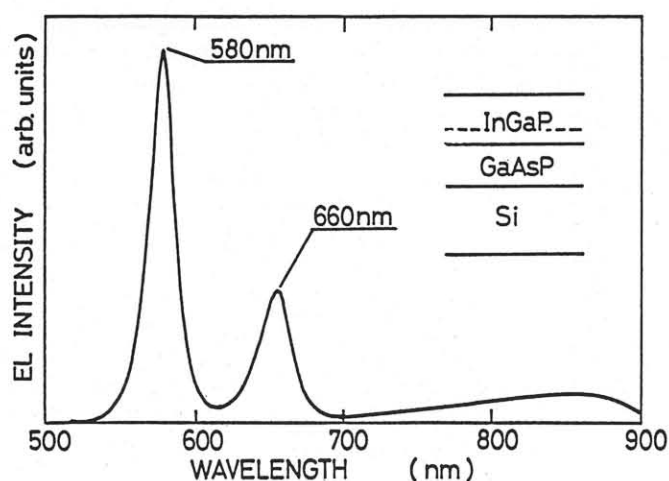


Fig.9 Emitting spectra at 580 nm from an InGaP/GaAsP/Si LED.

the high injection current of  $5 \text{ kA/cm}^2$  for 10 hours. These facts show that it is reasonable to expect LEDs on Si substrates in the future.

LEDs with emission of 580nm were similarly fabricated on Si using GaAsP buffer layers. The LED spectrum is shown in Fig. 9. Emission at 660 nm was due to the carrier injection into the GaAsP buffer layer because the p-n junction was very close to the GaAsP/InGaP interface in this case.

For improving LED performance, growth of thick InGaP films on Si substrates is important. For this purpose, InGaP layer was selectively grown on Si by patterning the GaAs buffer layer. The InGaP layer grew only on the GaAs surface because of a thin naturally formed oxide film on the Si surface. A SEM view of the selective growth wafer is shown in Fig. 10. Crack free InGaP of about  $6 \mu\text{m}$  thickness was grown easily.

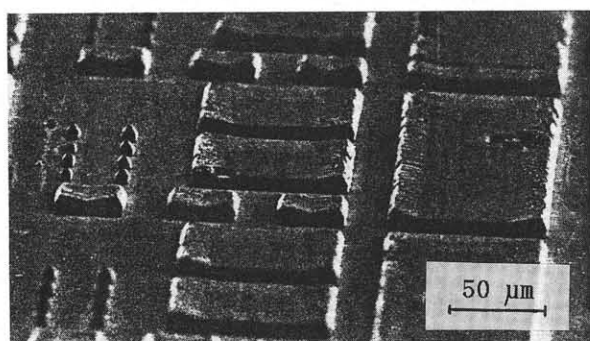


Fig.10 SEM view of the selectively grown InGaP/GaAs/Si structure.

#### 4. Summary

InGaP LEDs operating at 660 nm and 580 nm were fabricated on Si substrates. The InGaP layers were grown by M0-chloride VPE on MOVPE grown GaAs and GaAsP buffer layers. Optical and electrical characteristics of these LEDs show the feasibility of InGaP optical devices on Si substrates.

#### Acknowledgments

The authors would like to thank M.Ikeda for his helpful assistance and M.Yamaguchi, S.Miyazawa, T.Ikegami and M.Fujimoto for encouragement throughout this work.

#### References

- (1) T.Nonaka, M.Akiyama, Y.Kawarada and K.Kaminisi, Jpn.J.Appl.Phys. **23**, (1984) L919
- (2) Y.Itoh, T.Nishioka, A.Yamamoto and M.Yamaguchi, Appl.Phys.Lett. **49**, (1986) 1614; Appl.Phys.Lett. **52**, (1988) 1617
- (3) H.Z.Chen, A.Ghaffari, H.Wang, H.Morkoc and A.Yariv, Appl.Phys.Lett. **51**, (1987) 1320
- (4) D.G.Deppe, D.W.Nam, N.Holonyak, K.C.Hsieh, R.J.Maty, H.Shichijo, J.E.Epler and H.F.Chung, Appl.Phys. Lett. **51**, (1987) 1271
- (5) S.Kondo, S.Matsumoto and H.Nagai, to be published in Appl. Phys. Lett. (1988)
- (6) A.Hashimoto, Y.Kawarada, T.Kamijo, M.Akiyama, N.Watanabe and M.Sakuta, Appl.Phys.Lett. **48**, (1986) 1617
- (7) H.Mori, M.Ogasawara, M.Yamamoto and M.Tachikawa, Appl.Phys.Lett. **51**, 1245 (1987).
- (8) M.Ikeda, H.Sato, T.Ohta, K.Nakano, A.Toda, O.Kumagai and C.Kojima, Appl. Phys.Lett. **51**, 1572 (1976)
- (9) M.Yoshida, H.Terao and H.Watanabe, J. Electrochem. Soc.; solid. **132** (1985)
- (10) S.Kondo, T.Amano and H.Nagai, Jpn.J. Appl.Phys. **25**, L770 (1986)